TWMS J. App. and Eng. Math. V.15, N.11, 2025, pp. 2599-2612

FRACTIONAL CATTANEO EQUATION WITH A HARMONIC SOURCE AND ASSOCIATED THERMAL STRESSES IN AXISYMMETRIC AND CENTRAL SYMMETRIC CASES

V. KULKARNI[1*], S. SANKESHWARI[2], §

Abstract. Integer and fractional order Cattaneo equations with a source varying harmonically in time under zero initial conditions are studied in the axisymmetric case and the central symmetric case. The integral transform techniques are used to find the fundamental solutions. The displacement potential is used to find the associated thermal stresses in both cases. The impact of the fractional order parameters and time-harmonic source on the temperature as well as stress distributions has been examined. The outcomes of numerical computations are represented graphically for various values of the order of fractional derivatives. The main objective of the article is to examine the role of the order of the fractional derivatives in the rate of heat transfer and related thermal stresses. Moreover, it has been observed that the angular frequency controls the oscillatory behavior of solutions and also affects the amplitude of the oscillations. This analysis has a wide scope of applications in the study of viscoelastic materials, thermal energy storage systems, biological systems, etc.

Keywords: Cattaneo equation, Thermal stresses, Time harmonic impact, Non-Fourier heat conduction, Caputo derivative.

AMS Subject Classification: 26A33, 35L35, 44A10, 65R10, 74F05.

1. Introduction

The heat equation with the time-harmonic influence was initially examined by Angstrom [1]. To address a broad range of diffusion-related periodic phenomena, Mandelis [8] developed a unified mathematical framework. Vrentas [24] used the diffusion and mass transfer theory to solve a variety of transport problems. Oscillations can be introduced into the parabolic heat conduction equation in two distinct methods. In the first method, the harmonic source term is used by Nowacki [12], while in the second method, time-harmonic boundary conditions are used by Carslaw and Jaeger [4] and Morse and Feshbach [9].

[1] Department of Mathematics, University of Mumbai, Mumbai, 400 098, Maharashtra, India.
e-mail: drvinayaksk1@gmail.com; ORCID: 0000-0002-2507-4458.
[2] School of Mathematics, Applied Statistics and Analytics, NMIMS Deemed to be University, Navi Mumbai, 410 210, Maharashtra, India.
e-mail: sagarsankeshwari1@gmail.com; ORCID: 0000-0002-7482-5684.
[*] Corresponding author.
§ Manuscript received: September 19, 2024; accepted: January 15, 2025.
TWMS Journal of Applied and Engineering Mathematics, Vol.15, No.11;

Povstenko [16] investigated the fractional heat conduction equation with a time-harmonic source at the boundary. Zhu [25] simultaneously measured the thermal diffusivity and conductivity of graphite sheets using the heat-loss modified Angstrom method. The fractional heat equation with a time-harmonic source and associated thermal stresses were investigated by Povstenko [17]. Povstenko [18] discussed the fractional heat conduction equation and associated theories of thermoelasticity. The Cattaneo equation with a time-harmonic source in the Cartesian domain was discussed by Povstenko and Ostoja-Starzewski [19]. Povstenko [15] studied the non-homogeneous Cattaneo equation with the Caputo fractional derivative and generalized thermoelasticity in one dimensional and axisymmetric cases. On a real line, Povstenko and Ostoja-Starzewski [20] studied the telegraph equation in the context of the Caputo fractional derivative under a moving time-harmonic source. Povstenko et al. [21] studied the telegraph equation under a moving time-harmonic source in polar coordinates.

Nikan et al. [10] obtained a solution of the Cattaneo equation in the context of the Caputo fractional derivative of order $\alpha \in (1, 2)$ in a porous medium. Nikan et al. [11] obtained a solution for the time fractional Black–Scholes equation for American and European option pricing models. Avazzadeh et al. [2] studied the fractional Rayleigh–Stokes problem in a viscoelastic fluid by applying the localized hybrid kernel meshless technique. Luo et al. [7] proposed the Crank-Nicolson ADI Galerkin approach for obtaining a solution of the nonlocal heat model in three dimensions.

Physical processes take place at multiple structural levels. Memory effects are a physical concept that can be represented mathematically using fractional calculus. Our research focused on temperature and stress distributions and how they evolved, with special emphasis on the significance of the fractional order time derivative and time-harmonic heat source. Numerical results provided insights into the behavior of the obtained solutions, showing the impact of the fractional order parameter and harmonic source on the temperature as well as stress distributions.

The fractional Cattaneo equation with a time-harmonic source accurately models thermal stresses in axisymmetric and central symmetric geometries. It enables design optimization of thermal systems by accurately modeling thermal stresses and thermal waves. It improves predictions of thermal stresses, reducing the risk of thermal failure in engineering applications. The finite speed of thermal wave propagation was achieved due to the non-Fourier effect of heat conduction when $\alpha \to 1$. The role of the order of the fractional derivatives was examined in the rate of heat transfer and related thermal effects. This analysis has a wide scope of applications in the medical sciences.

In the present article, basic equations are mentioned in Section 2. In sections 3 and 4, the solutions of the integer order Cattaneo equation and the fractional Cattaneo equation are obtained, and the associated thermal stresses are investigated in the axisymmetric case and the central symmetric case respectively. The obtained results are represented graphically. The conclusions are drawn in Section 5.

2. Basic Equations

The non-classical heat conduction is represented by Cattaneo [5] and Vernotte [23] of the form

$$\mathbf{q} + \tau_0 \frac{\partial \mathbf{q}}{\partial t} = -\kappa \text{ grad } T, \tag{1}$$

where τ_0 denotes the relaxation time in the heat flux and is a non-negative constant, and κ represents the thermal conductivity of the material.

Combining equation (1) with a law of conservation of energy gives

$$\frac{\partial T}{\partial t} + \tau_0 \frac{\partial^2 T}{\partial t^2} = a\Delta T, \tag{2}$$

where a denotes the thermal diffusivity of the material.

Following Povstenko [15], the generalization of equation (1) in the context of the time fractional derivatives is given by

$$I^{1-\alpha}\mathbf{q} + \tau_0 \frac{\partial^\alpha \mathbf{q}}{\partial t^\alpha} = -\kappa \text{ grad } T, \qquad 0 < \alpha \le 1. \tag{3}$$

Combining equation (3) with a law of conservation of energy gives to the fractional Cattaneo equation as

$$\frac{\partial^\alpha T}{\partial t^\alpha} + \tau_0 \frac{\partial^{1+\alpha} T}{\partial t^{1+\alpha}} = a\Delta T, \qquad 0 < \alpha \le 1, \tag{4}$$

where

$$\frac{d^\alpha f}{dt^\alpha} = \begin{cases} \dfrac{1}{\Gamma(n-\alpha)} \displaystyle\int_0^t \frac{f^n(\xi)}{\big(t-\xi\big)^{\alpha+1-n}} d\xi, & n-1 < \alpha < n, \\ f^n(\xi), & \alpha = n, \end{cases} \tag{5}$$

represents the Caputo fractional derivative of order α [6, 22]. The above equation (4) is parabolic if $\alpha \to 0$ and hyperbolic if $\alpha \to 1$.

3. Axisymmetric case

3.1. **Integer order Cattaneo equation.** Consider the Cattaneo equation with a harmonic source as

$$\frac{\partial T}{\partial t} + \tau_0 \frac{\partial^2 T}{\partial t^2} = a\left(\frac{\partial^2 T}{\partial r^2} + \frac{1}{r}\frac{\partial T}{\partial r}\right) + \frac{q_0 \delta(r) e^{i\omega t}}{2\pi r}, \quad 0 \le r < \infty, \tag{6}$$

where ω is the angular frequency.

Initially

$$T = \frac{\partial T}{\partial t} = 0 \text{ at } t = 0. \tag{7}$$

The nondimensional quantities listed below have been introduced in equation (6)

$$\bar{t} = \frac{t}{t_0},\ \bar{\omega} = t_0\omega,\ \bar{r} = \frac{r}{t_0^{1/2}\sqrt{a}},\ \bar{\tau_0} = \frac{\tau_0}{t_0},\ \bar{T} = \frac{aT}{q_0},\ \bar{\sigma_{ij}} = \frac{a}{2\mu m q_0}\sigma_{ij}, \tag{8}$$

where t_0 is the characteristic time.

In the view of nondimensional quantities, equation (6) can be converted into nondimensional form as

$$\frac{\partial \bar{T}}{\partial \bar{t}} + \bar{\tau_0}\frac{\partial^2 \bar{T}}{\partial \bar{t}^2} = \left(\frac{\partial^2 \bar{T}}{\partial \bar{r}^2} + \frac{1}{\bar{r}}\frac{\partial \bar{T}}{\partial \bar{r}}\right) + \frac{\delta(\bar{r}) e^{i\bar{\omega}\bar{t}}}{2\pi \bar{r}}, \tag{9}$$

Operating the Laplace transform operator $\mathscr{L}$ to equation (9)

$$\mathscr{L}\left\{\frac{\partial \bar{T}}{\partial \bar{t}} + \bar{\tau_0}\frac{\partial^2 \bar{T}}{\partial \bar{t}^2}\right\} = \mathscr{L}\left\{\left(\frac{\partial^2 \bar{T}}{\partial \bar{r}^2} + \frac{1}{\bar{r}}\frac{\partial \bar{T}}{\partial \bar{r}}\right) + \frac{\delta(\bar{r}) e^{i\bar{\omega}\bar{t}}}{2\pi \bar{r}}\right\}, \tag{10}$$

Equation (10) reduces to the following form

$$\big(p + \bar{\tau_0}p^2\big)\hat{\bar{T}} = \frac{\partial^2 \hat{\bar{T}}}{\partial \bar{r}^2} + \frac{1}{\bar{r}}\frac{\partial \hat{\bar{T}}}{\partial \bar{r}} + \frac{\delta(\bar{r})}{2\pi\bar{r}(p - i\bar{\omega})}, \tag{11}$$

where p denotes the Laplace transform parameter, and hat denotes the Laplace transform.

Operating the Hankel transform operator $\mathscr{H}$ to equation (11)

$$\mathscr{H}\left\{\left(p+\bar{\tau}_0 p^2\right)\hat{\bar{T}}\right\} = \mathscr{H}\left\{\frac{\partial^2\hat{\bar{T}}}{\partial\bar{r}^2} + \frac{1}{\bar{r}}\frac{\partial\hat{\bar{T}}}{\partial\bar{r}} + \frac{\delta(\bar{r})}{2\pi\bar{r}(p-i\bar{\omega})}\right\}, \tag{12}$$

Equation (12) acquires in the transform domain as

$$\hat{\bar{T}}^*(\eta, p) = \frac{1}{2\pi(p-i\bar{\omega})\left(p+\bar{\tau}_0 p^2+\eta^2\right)}, \tag{13}$$

where η denotes the Hankel transform parameter, and an asterisk denotes the Hankel transform.

Let

$$F(p) = \frac{1}{p+\bar{\tau}_0 p^2+\eta^2} \text{ and } G(p) = \frac{1}{p-i\bar{\omega}}. \tag{14}$$

To find the inverse Laplace transform of $F(p)$ and $G(p)$.

Let

$$f(\bar{t}, \bar{\tau}_0, \eta) = \mathscr{L}^{-1}\left(\frac{1}{p+\bar{\tau}_0 p^2+\eta^2}\right) = \frac{1}{2\pi i}\int_{c-i\infty}^{c+i\infty}\frac{e^{p\bar{t}}}{p+\bar{\tau}_0 p^2+\eta^2}dp. \tag{15}$$

To evaluate the integral equation (15) by using the residue theorem

$$f(\bar{t}, \bar{\tau}_0, \eta) = \frac{e^{p_1\bar{t}} - e^{p_2\bar{t}}}{p_1-p_2}, \text{ where } p_1 = \frac{\frac{-1}{\bar{\tau}_0} + \sqrt{\frac{1}{\bar{\tau}_0{}^2} - \frac{4\eta^2}{\bar{\tau}_0}}}{2}, \; p_2 = \frac{\frac{-1}{\bar{\tau}_0} - \sqrt{\frac{1}{\bar{\tau}_0{}^2} - \frac{4\eta^2}{\bar{\tau}_0}}}{2} \tag{16}$$

and

$$\mathscr{L}^{-1}\big[G(p)\big] = \mathscr{L}^{-1}\left(\frac{1}{p-i\bar{\omega}}\right) = e^{i\bar{\omega}\bar{t}} = g(\bar{t}). \tag{17}$$

Operating the inverse Laplace transform operator $\mathscr{L}^{-1}$ to equation (13)

$$\mathscr{L}^{-1}\left\{\hat{\bar{T}}^*(\eta, p)\right\} = \mathscr{L}^{-1}\left\{\frac{1}{2\pi(p-i\bar{\omega})\left(p+\bar{\tau}_0 p^2+\eta^2\right)}\right\}, \tag{18}$$

Using equations (16) – (17) and the convolution theorem, one becomes

$$\bar{T}^*(\eta, \bar{t}) = \frac{1}{2\pi}\int_0^{\bar{t}}\frac{e^{p_1 u} - e^{p_2 u}}{p_1-p_2}e^{i\bar{\omega}(\bar{t}-u)}\, du, \tag{19}$$

Operating the inverse Hankel transform operator $\mathscr{H}^{-1}$ to equation (19)

$$\mathscr{H}^{-1}\left\{\bar{T}^*(\eta, \bar{t})\right\} = \mathscr{H}^{-1}\left\{\frac{1}{2\pi}\int_0^{\bar{t}}\frac{e^{p_1 u} - e^{p_2 u}}{p_1-p_2}e^{i\bar{\omega}(\bar{t}-u)}\, du\right\}, \tag{20}$$

On simplifying equation (20) leads to the solution as

$$\bar{T}(\bar{r}, \bar{t}) = \frac{1}{2\pi}\int_0^{\bar{t}}\int_0^{\infty}\frac{e^{p_1 u} - e^{p_2 u}}{p_1-p_2}e^{i\bar{\omega}(\bar{t}-u)}J_0(\bar{r}\eta)\; \eta\; d\eta\; du, \tag{21}$$

where $J_0(z)$ is the Bessel function.

3.2. **Fractional Cattaneo equation.** Consider the fractional Cattaneo equation with a harmonic source as

$$\frac{\partial^{\alpha} T}{\partial t^{\alpha}} + \tau_0 \frac{\partial^{1+\alpha} T}{\partial t^{1+\alpha}} = a\left(\frac{\partial^2 T}{\partial r^2} + \frac{1}{r}\frac{\partial T}{\partial r}\right) + \frac{q_0 \delta(r) e^{i\omega t}}{2\pi r}, \quad 0 \le r < \infty. \tag{22}$$

Equation (22) is studied under zero initial conditions as given in equation (7).

The nondimensional quantities listed below have been introduced in equation (22)

$$\bar{t} = \frac{t}{t_0},\ \bar{\omega} = t_0 \omega,\ \bar{r} = \frac{r}{t_0^{\alpha/2}\sqrt{a}},\ \bar{\tau_0} = \frac{\tau_0}{t_0},\ \bar{T} = \frac{aT}{q_0},\ \bar{\sigma_{ij}} = \frac{a}{2\mu m q_0}\sigma_{ij}, \tag{23}$$

where t_0 is the characteristic time.

In the view of nondimensional quantities, equation (22) can be converted into nondimensional form as

$$\frac{\partial^{\alpha} \bar{T}}{\partial \bar{t}^{\alpha}} + \bar{\tau_0} \frac{\partial^{1+\alpha} \bar{T}}{\partial \bar{t}^{1+\alpha}} = \left(\frac{\partial^2 \bar{T}}{\partial \bar{r}^2} + \frac{1}{\bar{r}}\frac{\partial \bar{T}}{\partial \bar{r}}\right) + \frac{\delta(\bar{r}) e^{i\bar{\omega}\bar{t}}}{2\pi \bar{r}}, \tag{24}$$

Operating the Laplace transform operator $\mathscr{L}$ to equation (24)

$$\mathscr{L}\left\{\frac{\partial^{\alpha} \bar{T}}{\partial \bar{t}^{\alpha}} + \bar{\tau_0} \frac{\partial^{1+\alpha} \bar{T}}{\partial \bar{t}^{1+\alpha}}\right\} = \mathscr{L}\left\{\left(\frac{\partial^2 \bar{T}}{\partial \bar{r}^2} + \frac{1}{\bar{r}}\frac{\partial \bar{T}}{\partial \bar{r}}\right) + \frac{\delta(\bar{r}) e^{i\bar{\omega}\bar{t}}}{2\pi \bar{r}}\right\}, \tag{25}$$

Equation (25) converts into the following form

$$\left(p^{\alpha} + \bar{\tau_0} p^{1+\alpha}\right)\hat{\bar{T}} = \frac{\partial^2 \hat{\bar{T}}}{\partial \bar{r}^2} + \frac{1}{\bar{r}}\frac{\partial \hat{\bar{T}}}{\partial \bar{r}} + \frac{\delta(\bar{r})}{2\pi \bar{r}(p - i\bar{\omega})}, \tag{26}$$

where p denotes the Laplace transform parameter, and hat denotes the Laplace transform.

Operating the Hankel transform operator $\mathscr{H}$ to equation (26)

$$\mathscr{H}\left\{\left(p^{\alpha} + \bar{\tau_0} p^{1+\alpha}\right)\hat{\bar{T}}\right\} = \mathscr{H}\left\{\frac{\partial^2 \hat{\bar{T}}}{\partial \bar{r}^2} + \frac{1}{\bar{r}}\frac{\partial \hat{\bar{T}}}{\partial \bar{r}} + \frac{\delta(\bar{r})}{2\pi \bar{r}(p - i\bar{\omega})}\right\}, \tag{27}$$

Equation (27) results in the transform domain as

$$\hat{\bar{T}}^{*}(\eta, p) = \frac{1}{2\pi(p - i\bar{\omega})(p^{\alpha} + \bar{\tau_0} p^{1+\alpha} + \eta^2)}, \tag{28}$$

where η denotes the Hankel transform parameter, and an asterisk denotes the Hankel transform.

The transformation of the Bromwich path to the Hankel path is a mathematical technique used to evaluate the inverse Laplace transform. This transformation is valid under analyticity and no singularities conditions. To find the inverse Laplace transform, one bends the Bromwich path into the equivalent Hankel path [3], and then by using the residue theorem, one gets

$$\begin{aligned}\mathscr{L}^{-1}\left(\frac{1}{p^{\alpha} + \bar{\tau_0} p^{1+\alpha} + \eta^2}\right) &= G_{\alpha}\left(\bar{t}, \bar{\tau_0}, \eta\right) = \frac{1}{\pi}\int_0^{\infty} \mathrm{e}^{-z\bar{t}} \frac{S(z)}{\left[C(z)\right]^2 + \left[S(z)\right]^2} dz \\ &+ \frac{2\mathrm{e}^{-\Psi\bar{t}}}{A^2 + B^2}\left[A\cos\left(\Omega\bar{t}\right) + B\sin\left(\Omega\bar{t}\right)\right],\end{aligned} \tag{29}$$

where $C(z) = \left(-\bar{\tau_0} z^{1+\alpha} + z^{\alpha}\right)\cos\left(\pi\alpha\right) + \eta^2$, $S(z) = \left(-\bar{\tau_0} z^{1+\alpha} + z^{\alpha}\right)\sin\left(\pi\alpha\right)$, $p_{1,2} = -\Psi \pm i\Omega$ are simple, conjugate complex zeros of $p^{\alpha} + \bar{\tau_0} p^{1+\alpha} + \eta^2$ on the principal branch of p^{α} $\left(-\pi < \arg p < \pi\right)$. These are located in $\Omega > 0$ and $\Psi > 0$, whereas $A \pm iB = (1+\alpha)\bar{\tau_0} p_{1,2}^{\alpha} + \alpha p_{1,2}^{\alpha-1}$.

Operating the inverse Laplace transform operator $\mathscr{L}^{-1}$ to equation (28)

$$\mathscr{L}^{-1}\left\{\hat{\bar{T}}^{*}(\eta,p)\right\}=\mathscr{L}^{-1}\left\{\frac{1}{2\pi(p-i\bar{\omega})(p^{\alpha}+\bar{\tau}_{0}p^{1+\alpha}+\eta^{2})}\right\}, \tag{30}$$

After inverting the transform, equation (30) achieves the form as

$$\bar{T}^{*}(\eta,\bar{t})=\frac{1}{2\pi}\int_{0}^{\bar{t}}G_{\alpha}(u,\bar{\tau}_{0},\eta)\ \mathrm{e}^{i\bar{\omega}(\bar{t}-u)}\ du, \tag{31}$$

Operating the inverse Hankel transform operator $\mathscr{H}^{-1}$ to equation (31)

$$\mathscr{H}^{-1}\left\{\bar{T}^{*}(\eta,\bar{t})\right\}=\mathscr{H}^{-1}\left\{\frac{1}{2\pi}\int_{0}^{\bar{t}}G_{\alpha}(u,\bar{\tau}_{0},\eta)\ \mathrm{e}^{i\bar{\omega}(\bar{t}-u)}\ du\right\}, \tag{32}$$

On solving equation (32) gives the solution as

$$\bar{T}(\bar{r},\bar{t})=\frac{1}{2\pi}\int_{0}^{\bar{t}}\int_{0}^{\infty}G_{\alpha}(u,\bar{\tau}_{0},\eta)\ \mathrm{e}^{i\bar{\omega}(\bar{t}-u)}J_{0}(\bar{r}\eta)\ \eta\ d\eta\ du. \tag{33}$$

All computations were carried out in MATLAB R2022a on a desktop computer with an Intel Core i3-1005G1 processor, 1.2 GHz, and 8GB RAM, running 64-bit Windows 11. The outcomes of the numerical computation of the real part of the solution (33) are shown in Figures 1 and 2 for distinct values of fractional order α and nondimensional parameters (23). The curve for $\alpha = 1$ in these figures is corresponding to equation (21). Figure 1 shows that temperature $\bar{T}(\bar{r},\bar{t})$ increases when fractional order α decreases along radial coordinate $\bar{r}$. Figure 2 shows that temperature $\bar{T}(\bar{r},\bar{t})$ is attaining positive and negative values along angular frequency $\bar{\omega}$.

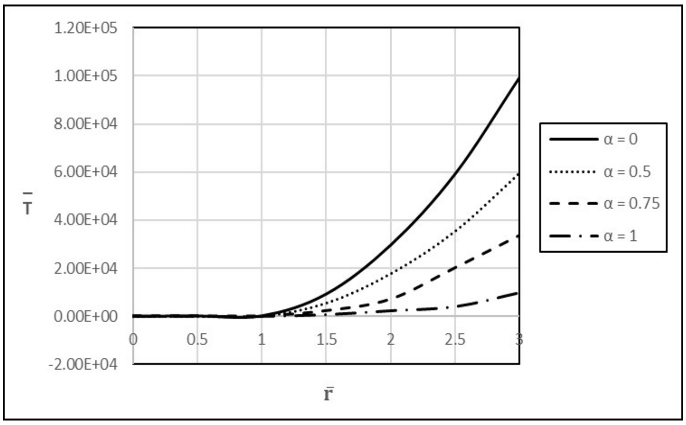

FIGURE 1. Temperature variation with respect to fractional order α along radial coordinate $\bar{r}$ when $\bar{\tau}_0 = 0.5$, $\bar{w} = \pi/4$.

3.3. **Thermal Stresses.** The displacement potential is used to find the stress tensor components [13, 14]. The potential Φ satisfies the following

$$\nabla^{2}\Phi=mT, \tag{34}$$

where $m = (1+\nu)\alpha_t/(1-\nu)$, μ denotes the Lamé constant, and ν is the Poisson ratio.

Knowing the function Φ to determine the stress components from

$$\sigma_{ij}=2\mu\left(\frac{\partial^{2}\Phi}{\partial i\partial j}-\nabla^{2}\Phi\delta_{ij}\right),\quad i,j=x,y,z, \tag{35}$$

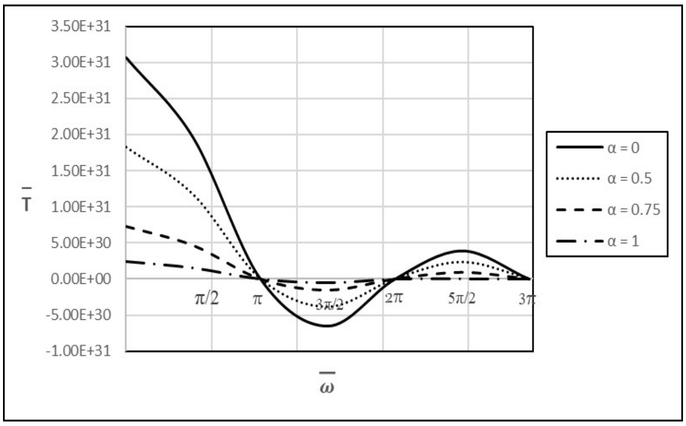

FIGURE 2. Temperature variation with respect to fractional order α along angular frequency $\bar{\omega}$ when $\bar{\tau}_0 = 0.5$, $\bar{r} = 1$.

where δ_{ij} is Kronecker's delta.

The stress tensor components are

$$\bar{\sigma}_{rr} + \bar{\sigma}_{\theta\theta} = -\frac{1}{2\pi} \int_0^{\bar{t}} \int_0^{\infty} G_\alpha(u, \bar{\tau}_0, \eta)\ \mathrm{e}^{i\bar{\omega}(\bar{t}-u)} J_0(\bar{r}\eta)\ \eta\ d\eta\ du, \tag{36}$$

$$\bar{\sigma}_{rr} - \bar{\sigma}_{\theta\theta} = -\frac{1}{2\pi} \int_0^{\bar{t}} \int_0^{\infty} G_\alpha(u, \bar{\tau}_0, \eta)\ \mathrm{e}^{i\bar{\omega}(\bar{t}-u)} J_2(\bar{r}\eta)\ \eta\ d\eta\ du, \tag{37}$$

or

$$\bar{\sigma}_{rr} = -\frac{1}{2\pi\bar{r}} \int_0^{\bar{t}} \int_0^{\infty} G_\alpha(u, \bar{\tau}_0, \eta)\ \mathrm{e}^{i\bar{\omega}(\bar{t}-u)} J_1(\bar{r}\eta)\ d\eta\ du, \tag{38}$$

$$\bar{\sigma}_{\theta\theta} = -\bar{T} - \bar{\sigma}_{rr}. \tag{39}$$

The outcomes of the numerical computation of the real part of the solutions (38) and (39) are shown in Figures 3 and 4 for distinct values of fractional order α and nondimensional parameters. From both figures, it has been observed that stress values $\bar{\sigma}_{rr}, \bar{\sigma}_{\theta\theta}$ decrease when fractional order α decreases along radial coordinate $\bar{r}$.

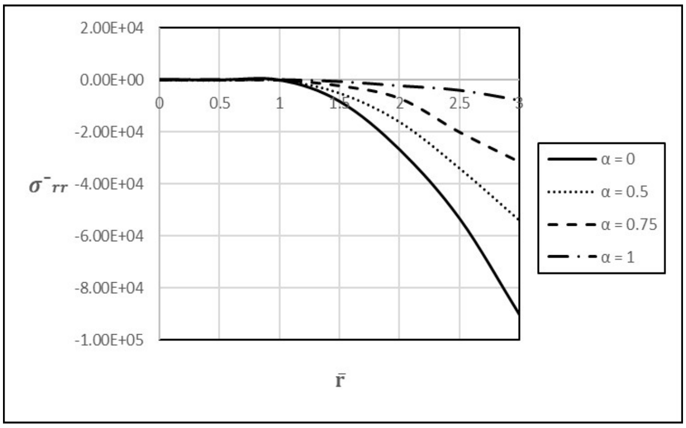

FIGURE 3. Stress variation $\bar{\sigma}_{rr}$ with respect to fractional order α along radial coordinate $\bar{r}$ when $\bar{\tau}_0 = 0.5$, $\bar{w} = \pi/4$.

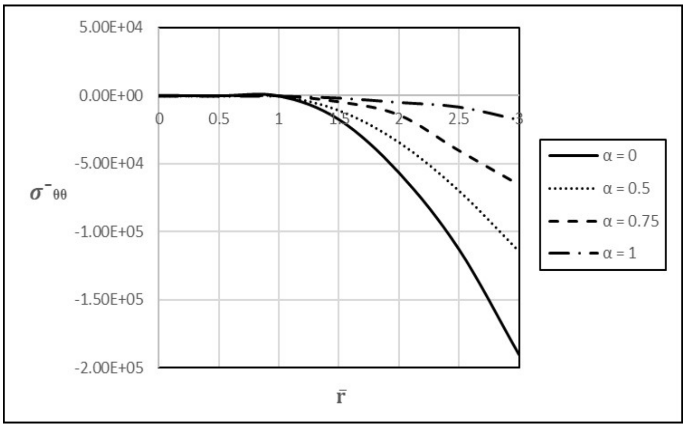

FIGURE 4. Stress variation $\bar{\sigma}_{\theta\theta}$ with respect to fractional order α along radial coordinate $\bar{r}$ when $\bar{\tau_0} = 0.5$, $\bar{w} = \pi/4$.

4. Central Symmetric Case

4.1. **Integer order Cattaneo equation.** Consider the Cattaneo equation with a harmonic source as

$$\frac{\partial T}{\partial t} + \tau_0 \frac{\partial^2 T}{\partial t^2} = a\left(\frac{\partial^2 T}{\partial r^2} + \frac{2}{r}\frac{\partial T}{\partial r}\right) + \frac{q_0 \delta(r) e^{i\omega t}}{4\pi r^2}, \quad 0 \le r < \infty, \tag{40}$$

where ω is the angular frequency.

Equation (40) is studied under zero initial conditions as given in equation (7).

The nondimensional quantities listed below have been introduced in equation (40)

$$\bar{t} = \frac{t}{t_0},\ \bar{\omega} = t_0\omega,\ \bar{r} = \frac{r}{t_0^{1/2}\sqrt{a}},\ \bar{\tau_0} = \frac{\tau_0}{t_0},\ \bar{T} = \frac{a^{3/2} t_0^{\alpha/2}}{q_0} T,\ \bar{\sigma_{ij}} = \frac{a^{3/2} t_0^{\alpha/2}}{2\mu m q_0}\sigma_{ij}, \tag{41}$$

where t_0 is the characteristic time.

In the view of nondimensional quantities, equation (40) can be converted into nondimensional form as

$$\frac{\partial \bar{T}}{\partial \bar{t}} + \bar{\tau_0}\frac{\partial^2 \bar{T}}{\partial \bar{t}^2} = \left(\frac{\partial^2 \bar{T}}{\partial \bar{r}^2} + \frac{2}{\bar{r}}\frac{\partial \bar{T}}{\partial \bar{r}}\right) + \frac{\delta(\bar{r}) e^{i\bar{\omega}\bar{t}}}{4\pi \bar{r}^2}, \tag{42}$$

Operating the Laplace transform operator $\mathscr{L}$ to equation (42)

$$\mathscr{L}\left\{\frac{\partial \bar{T}}{\partial \bar{t}} + \bar{\tau_0}\frac{\partial^2 \bar{T}}{\partial \bar{t}^2}\right\} = \mathscr{L}\left\{\left(\frac{\partial^2 \bar{T}}{\partial \bar{r}^2} + \frac{2}{\bar{r}}\frac{\partial \bar{T}}{\partial \bar{r}}\right) + \frac{\delta(\bar{r}) e^{i\bar{\omega}\bar{t}}}{4\pi \bar{r}^2}\right\}, \tag{43}$$

Equation (43) reduces to the following form

$$\left(p + \bar{\tau_0} p^2\right)\hat{\bar{T}} = \frac{\partial^2 \hat{\bar{T}}}{\partial \bar{r}^2} + \frac{2}{\bar{r}}\frac{\partial \hat{\bar{T}}}{\partial \bar{r}} + \frac{\delta(\bar{r})}{4\pi \bar{r}^2 (p - i\bar{\omega})}, \tag{44}$$

where p denotes the Laplace transform parameter, and hat denotes the Laplace transform.

Operating the Fourier transform operator $\mathscr{F}$ to equation (44)

$$\mathscr{F}\left\{\left(p + \bar{\tau_0} p^2\right)\hat{\bar{T}}\right\} = \mathscr{F}\left\{\frac{\partial^2 \hat{\bar{T}}}{\partial \bar{r}^2} + \frac{2}{\bar{r}}\frac{\partial \hat{\bar{T}}}{\partial \bar{r}} + \frac{\delta(\bar{r})}{4\pi \bar{r}^2 (p - i\bar{\omega})}\right\}, \tag{45}$$

Equation (45) acquires in the transform domain as

$$\hat{\bar{T}}^{*}(\xi,p)=\frac{1}{(2\pi)^{3/2}(p-i\bar{\omega})\,(p+\bar{\tau}_0p^2+\xi^2)},\tag{46}$$

where ξ is the Fourier transform parameter, and an asterisk denotes the Fourier transform.

Operating the inverse Laplace transform operator $\mathscr{L}^{-1}$ to equation (46)

$$\mathscr{L}^{-1}\left\{\hat{\bar{T}}^{*}(\xi,p)\right\}=\mathscr{L}^{-1}\left\{\frac{1}{(2\pi)^{3/2}(p-i\bar{\omega})\,(p+\bar{\tau}_0p^2+\xi^2)}\right\},\tag{47}$$

Using equations (16) – (17) and the convolution theorem, one becomes

$$\bar{T}^{*}(\xi,\bar{t})=\frac{1}{(2\pi)^{3/2}}\int_0^{\bar{t}}\frac{e^{p_1u}-e^{p_2u}}{p_1-p_2}e^{i\bar{\omega}(\bar{t}-u)}\,du,\tag{48}$$

Operating the inverse Fourier transform operator $\mathscr{F}^{-1}$ to equation (48)

$$\mathscr{F}^{-1}\left\{\bar{T}^{*}(\xi,\bar{t})\right\}=\mathscr{F}^{-1}\left\{\frac{1}{(2\pi)^{3/2}}\int_0^{\bar{t}}\frac{e^{p_1u}-e^{p_2u}}{p_1-p_2}e^{i\bar{\omega}(\bar{t}-u)}\,du\right\},\tag{49}$$

On simplifying equation (49) leads to the solution as

$$\bar{T}(\bar{r},\bar{t})=\frac{1}{2\pi^2}\int_0^{\bar{t}}\int_0^{\infty}\frac{e^{p_1u}-e^{p_2u}}{p_1-p_2}e^{i\bar{\omega}(\bar{t}-u)}\frac{\sin(\bar{r}\xi)}{\bar{r}}\;\xi\;d\xi\;du.\tag{50}$$

4.2. **Fractional Cattaneo equation.** Consider the fractional Cattaneo equation with a harmonic source as

$$\frac{\partial^{\alpha}T}{\partial t^{\alpha}}+\tau_0\frac{\partial^{1+\alpha}T}{\partial t^{1+\alpha}}=a\left(\frac{\partial^2T}{\partial r^2}+\frac{2}{r}\frac{\partial T}{\partial r}\right)+\frac{q_0\delta(r)e^{i\omega t}}{4\pi r^2},\quad 0\le r<\infty,\tag{51}$$

Equation (51) is studied under zero initial conditions as given in equation (7).

The nondimensional quantities listed below have been introduced in equation (51)

$$\bar{t}=\frac{t}{t_0},\ \bar{\omega}=t_0\omega,\ \bar{r}=\frac{r}{t_0^{\alpha/2}\sqrt{a}},\ \bar{\tau_0}=\frac{\tau_0}{t_0},\ \bar{T}=\frac{a^{3/2}t_0^{\alpha/2}}{q_0}T,\ \bar{\sigma_{ij}}=\frac{a^{3/2}t_0^{\alpha/2}}{2\mu m q_0}\sigma_{ij},\tag{52}$$

where t_0 is the characteristic time.

In the view of nondimensional quantities, equation (51) can be converted into nondimensional form as

$$\frac{\partial^{\alpha}\bar{T}}{\partial\bar{t}^{\alpha}}+\bar{\tau}_0\frac{\partial^{1+\alpha}\bar{T}}{\partial\bar{t}^{1+\alpha}}=\left(\frac{\partial^2\bar{T}}{\partial\bar{r}^2}+\frac{2}{\bar{r}}\frac{\partial\bar{T}}{\partial\bar{r}}\right)+\frac{\delta(\bar{r})e^{i\bar{\omega}\bar{t}}}{4\pi\bar{r}^2},\tag{53}$$

Operating the Laplace transform operator $\mathscr{L}$ to equation (53)

$$\mathscr{L}\left\{\frac{\partial^{\alpha}\bar{T}}{\partial\bar{t}^{\alpha}}+\bar{\tau}_0\frac{\partial^{1+\alpha}\bar{T}}{\partial\bar{t}^{1+\alpha}}\right\}=\mathscr{L}\left\{\left(\frac{\partial^2\bar{T}}{\partial\bar{r}^2}+\frac{2}{\bar{r}}\frac{\partial\bar{T}}{\partial\bar{r}}\right)+\frac{\delta(\bar{r})e^{i\bar{\omega}\bar{t}}}{4\pi\bar{r}^2}\right\},\tag{54}$$

Equation (54) converts into the following form

$$\left(p^{\alpha}+\bar{\tau}_0p^{1+\alpha}\right)\hat{\bar{T}}=\frac{\partial^2\hat{\bar{T}}}{\partial\bar{r}^2}+\frac{2}{\bar{r}}\frac{\partial\hat{\bar{T}}}{\partial\bar{r}}+\frac{\delta(\bar{r})}{4\pi\bar{r}^2(p-i\bar{\omega})},\tag{55}$$

where p denotes the Laplace transform parameter, and hat denotes the Laplace transform.

Operating the Fourier transform operator $\mathscr{F}$ to equation (55)

$$\mathscr{F}\left\{\left(p^{\alpha}+\bar{\tau}_0p^{1+\alpha}\right)\hat{\bar{T}}\right\}=\mathscr{F}\left\{\frac{\partial^2\hat{\bar{T}}}{\partial\bar{r}^2}+\frac{2}{\bar{r}}\frac{\partial\hat{\bar{T}}}{\partial\bar{r}}+\frac{\delta(\bar{r})}{4\pi\bar{r}^2(p-i\bar{\omega})}\right\},\tag{56}$$

Equation (56) results in the transform domain as

$$\hat{\bar{T}}^*(\xi,p)=\frac{1}{(2\pi)^{3/2}(p-i\bar{\omega})(p^\alpha+\bar{\tau}_0p^{1+\alpha}+\xi^2)},\tag{57}$$

where ξ denotes the Fourier transform parameter, and an asterisk denotes the Fourier transform.

To find the inverse Laplace transform, one bends the Bromwich path into the equivalent Hankel path [3], and then using the residue theorem, one obtains

$$\begin{aligned}\mathscr{L}^{-1}\left(\frac{1}{p^\alpha+\bar{\tau}_0p^{1+\alpha}+\xi^2}\right)&=G_\alpha\big(\bar{t},\bar{\tau}_0,\xi\big)=\frac{1}{\pi}\int_0^\infty \mathrm{e}^{-z\bar{t}}\frac{S(z)}{\big[C(z)\big]^2+\big[S(z)\big]^2}dz\\&+\frac{2\mathrm{e}^{-\Psi\bar{t}}}{A^2+B^2}\Big[A\cos\big(\Omega\bar{t}\big)+B\sin\big(\Omega\bar{t}\big)\Big],\end{aligned}\tag{58}$$

where $C(z)=\big(-\bar{\tau}_0z^{1+\alpha}+z^\alpha\big)\cos\big(\pi\alpha\big)+\xi^2$, $S(z)=\big(-\bar{\tau}_0z^{1+\alpha}+z^\alpha\big)\sin\big(\pi\alpha\big)$, $p_{1,2}=-\Psi\pm i\Omega$ are simple, conjugate complex zeros of $p^\alpha+\bar{\tau}_0p^{1+\alpha}+\xi^2$ on the principal branch of p^α $\big(-\pi<\arg p<\pi\big)$. These are located in $\Omega>0$ and $\Psi>0$, whereas $A\pm iB=(1+\alpha)\bar{\tau}_0p_{1,2}^\alpha+\alpha p_{1,2}^{\alpha-1}$.

Operating the inverse Laplace transform operator $\mathscr{L}^{-1}$ to equation (57)

$$\mathscr{L}^{-1}\Big\{\hat{\bar{T}}^*(\xi,p)\Big\}=\mathscr{L}^{-1}\Big\{\frac{1}{(2\pi)^{3/2}(p-i\bar{\omega})(p^\alpha+\bar{\tau}_0p^{1+\alpha}+\xi^2)}\Big\},\tag{59}$$

After inverting the transform, equation (59) achieves the form as

$$\bar{T}^*(\xi,\bar{t})=\frac{1}{(2\pi)^{3/2}}\int_0^{\bar{t}}G_\alpha(u,\bar{\tau}_0,\xi)\ \mathrm{e}^{i\bar{\omega}(\bar{t}-u)}\ du,\tag{60}$$

Operating the inverse Fourier transform operator $\mathscr{F}^{-1}$ to equation (60)

$$\mathscr{F}^{-1}\Big\{\bar{T}^*(\xi,\bar{t})\Big\}=\mathscr{F}^{-1}\Big\{\frac{1}{(2\pi)^{3/2}}\int_0^{\bar{t}}G_\alpha(u,\bar{\tau}_0,\xi)\ \mathrm{e}^{i\bar{\omega}(\bar{t}-u)}\ du\Big\},\tag{61}$$

On solving equation (61) gives the solution as

$$\bar{T}(\bar{r},\bar{t})=\frac{1}{2\pi^2}\int_0^{\bar{t}}\int_0^\infty G_\alpha(u,\bar{\tau}_0,\xi)\ \mathrm{e}^{i\bar{\omega}(\bar{t}-u)}\frac{\sin(\bar{r}\xi)}{\bar{r}}\ \xi\ d\xi\ du.\tag{62}$$

The outcomes of the numerical computation of the real part of the solution (62) are shown in Figures 5 and 6 for distinct values of fractional order α and nondimensional parameters (52). The curve for $\alpha=1$ in these figures is corresponding to equation (50). Figure 5 shows that temperature $\bar{T}(\bar{r},\bar{t})$ continuously increases when fractional order increases along radial coordinate $\bar{r}$. Figure 6 shows that temperature $\bar{T}(\bar{r},\bar{t})$ is attaining positive and negative values along angular frequency $\bar{\omega}$.

4.3. **Thermal Stresses.** The stress tensor components are

$$\bar{\sigma}_{rr}=\frac{1}{\pi^2}\int_0^{\bar{t}}\int_0^\infty G_\alpha(u,\bar{\tau}_0,\xi)\ \mathrm{e}^{i\bar{\omega}(\bar{t}-u)}\left[\frac{\bar{r}\xi\cos(\bar{r}\xi)-\sin(\bar{r}\xi)}{\xi\bar{r}^3}\right]\ d\xi\ du,\tag{63}$$

$$\bar{\sigma}_{\theta\theta}=\bar{\sigma}_{\phi\phi}=-2\bar{T}-\bar{\sigma}_{rr}.\tag{64}$$

The outcomes of the numerical computation of the real part of the solutions (63) and (64) are shown in Figures 7 to 9 for distinct values of fractional order α and nondimensional parameters. From all figures, it has been observed that stress values $\bar{\sigma}_{rr},\bar{\sigma}_{\theta\theta},\bar{\sigma}_{\phi\phi}$ are continuously increased and reached zero at the end when fractional order α increases along radial coordinate $\bar{r}$.

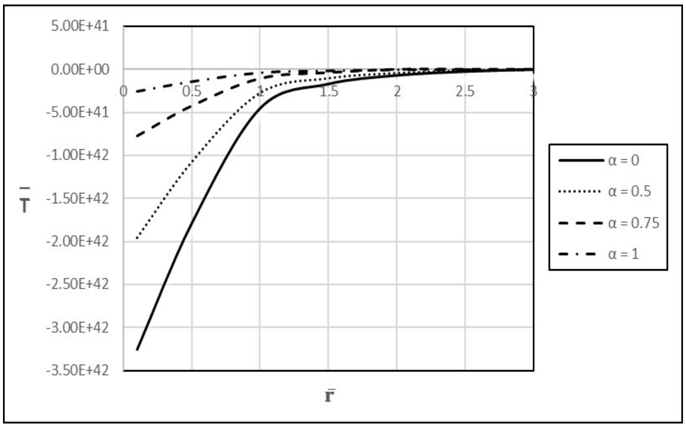

FIGURE 5. Temperature variation with respect to fractional order α along radial coordinate $\bar{r}$ when $\bar{\tau}_0 = 0.5$, $\bar{w} = \pi/4$.

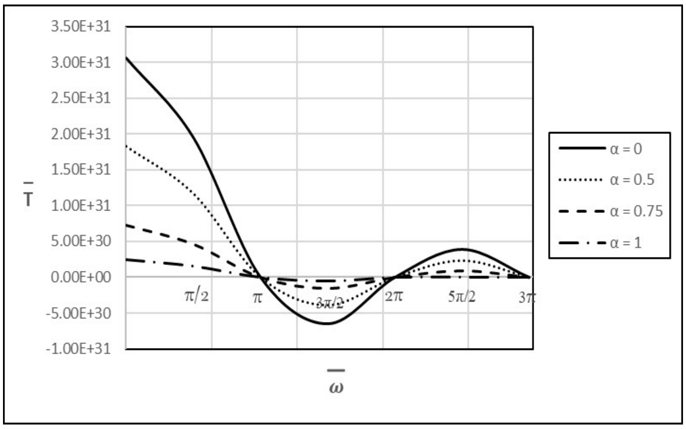

FIGURE 6. Temperature variation with respect to fractional order α along angular frequency $\bar{\omega}$ when $\bar{\tau}_0 = 0.5$, $\bar{r} = 1$.

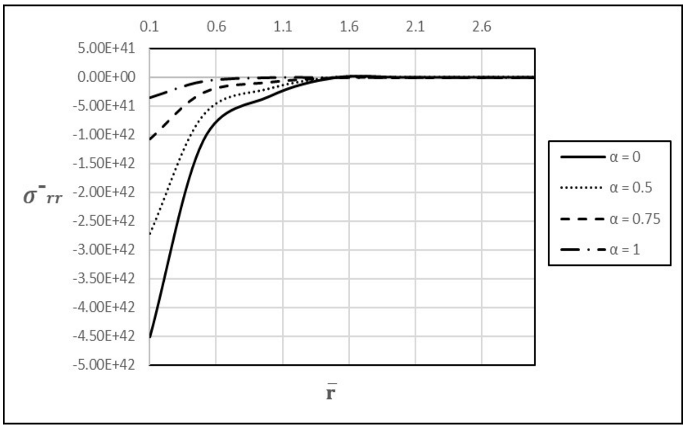

FIGURE 7. Stress variation $\bar{\sigma}_{rr}$ with respect to fractional order α along radial coordinate $\bar{r}$ when $\bar{\tau}_0 = 0.5$, $\bar{w} = \pi/4$.

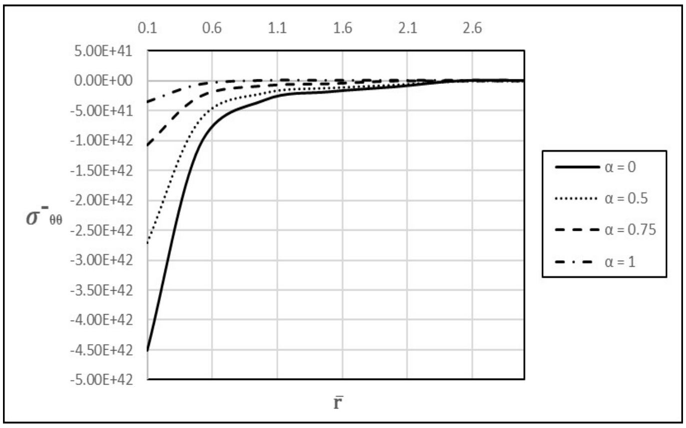

FIGURE 8. Stress variation $\bar{\sigma}_{\theta\theta}$ with respect to fractional order α along radial coordinate $\bar{r}$ when $\bar{\tau}_0 = 0.5$, $\bar{w} = \pi/4$.

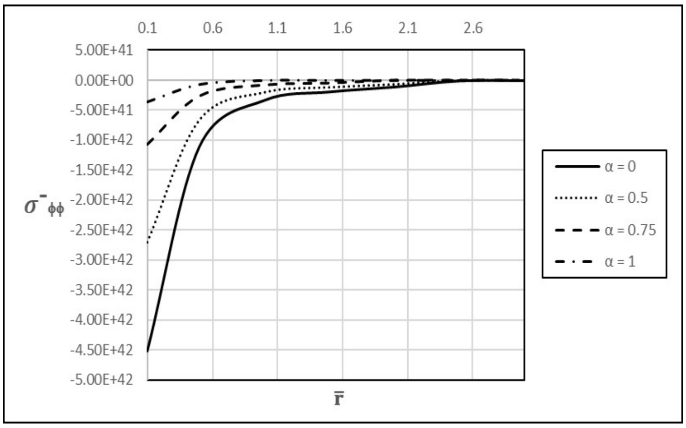

FIGURE 9. Stress variation $\bar{\sigma}_{\phi\phi}$ with respect to fractional order α along radial coordinate $\bar{r}$ when $\bar{\tau}_0 = 0.5$, $\bar{w} = \pi/4$.

5. Conclusions

The main outcomes are as follows:

(1) Integer and fractional order Cattaneo equations with a harmonic source were examined under zero initial conditions in axisymmetric and central symmetric cases. The solutions were achieved by applying the Laplace, Hankel, and Fourier transform techniques. The corresponding thermal stresses were also examined.
(2) To show the differences between the fractional model and the classical integer model, the solutions for various values of parameter α were shown in figures. The numerical results demonstrated the significant effect of parameter α on the temperature distribution along angular frequency and radial coordinate, as well as on stress distribution along the radial coordinate.
(3) According to numerical results, the fractional parameter evolved into a new measure of its ability to conduct thermal energy.
(4) The fractional order parameter controlled the memory effects. The angular frequency controlled the oscillatory behavior of solutions and also affected the amplitude of the oscillations.

(5) The finite speed of thermal wave propagation was attained by introducing the non-Fourier effect of heat conduction in the context of the relaxation time τ_0 when $\alpha \to 1$.
(6) The obtained solutions could be effectively used when the source term is expressed in the Fourier series form. The derived results could be used in medical science, such as in radioactive therapy, laser technology, flash burns of human skin, etc.
(7) The fractional Cattaneo equation with a harmonic source provided a versatile framework for understanding heat conduction in diverse materials and systems, especially those exhibiting anomalous or non-local thermal behavior. It had applications in various fields, including physics, engineering, and materials science.

Nomenclature

T	Absolute Temperature
r	Radial coordinate
t	Time
κ	Thermal conductivity
a	Thermal diffusivity of the material
τ_0	Relaxation time
t_0	Characteristic time
ω	Angular frequency
p	Laplace transform parameter
η	Hankel transform parameter
ξ	Fourier transform parameter
α	Fractional order
α_t	Coefficient of thermal expansion
μ	Lamé constant
ν	Poisson ratio
q_0	Constant heat flux
σ_{ij}	Components of stress tensor
Φ	Displacement Potential
δ_{ij}	Kronecker's delta
$\delta(r)$	Dirac delta function
Δ	Laplacian operator

References

[1] Angstrom, A. J., (1863), New method of determining the thermal conductibility of bodies, The London, Edinburgh, and Dublin Philosophical Magazine and Journal of Science, 25(166), pp. 130-142.
[2] Avazzadeh, Z., Nikan, O., Nguyen, A. T. and Nguyen, V. T., (2023), A localized hybrid kernel meshless technique for solving the fractional Rayleigh–Stokes problem for an edge in a viscoelastic fluid, Engineering Analysis with Boundary Elements, 146, pp. 695-705.
[3] Beyer, H. and Kempfle, S., (1995), Definition of physically consistent damping laws with fractional derivatives, ZAMM-Journal of Applied Mathematics and Mechanics/Zeitschrift für Angewandte Mathematik und Mechanik, 75(8), pp. 623-635.
[4] Carlsaw, H. S. and Jaeger, J. C., (1959), Conduction of heat in solids, Clarendon, Oxford.
[5] Cattaneo, C., (1958), Sur une forme de l'equation de la chaleur eliminant la paradoxe d'une propagation instantantee, Compt. Rendu, 247, pp. 431-433.
[6] Kilbas, A. A., Srivastava, H. M. and Trujillo, J. J., (2006), Theory and applications of fractional differential equations, elsevier.

[7] Luo, M., Qiu, W., Nikan, O. and Avazzadeh, Z., (2023), Second-order accurate, robust and efficient ADI Galerkin technique for the three-dimensional nonlocal heat model arising in viscoelasticity, Applied Mathematics and Computation, 440, p. 127655.
[8] Mandelis, A., (2013), Diffusion-wave fields: mathematical methods and Green functions, Springer Science and Business Media.
[9] Morse, P. M. and Feshbach, H., (1946), Methods of theoretical physics, Technology Press.
[10] Nikan, O., Avazzadeh, Z. and Machado, J. T., (2021), Numerical approach for modeling fractional heat conduction in porous medium with the generalized Cattaneo model, Applied Mathematical Modelling, 100, pp. 107-124.
[11] Nikan, O., Rashidinia, J. and Jafari, H., (2025), Numerically pricing American and European options using a time fractional Black–Scholes model in financial decision-making, Alexandria Engineering Journal, 112, pp. 235-245.
[12] Nowacki, W., (1957), State of stress in an elastic space due to a source of heat varying harmonically as function of time, Bull. Acad. Polon. Sci. Sér. Sci. Techn, 5(3), pp. 145-154.
[13] Nowacki, W., (1986), Thermoelasticity, 2nd edn, PWN.
[14] Parkus, H., (2013), Instationäre wärmespannungen, Springer-Verlag.
[15] Povstenko, Y. Z., (2011), Fractional Cattaneo-type equations and generalized thermoelasticity, Journal of thermal Stresses, 34(2), pp. 97-114.
[16] Povstenko, Y., (2016), Time-fractional heat conduction in a half-line domain due to boundary value of temperature varying harmonically in time, Mathematical Problems in Engineering, p. 2016.
[17] Povstenko, Y., (2016), Fractional heat conduction in a space with a source varying harmonically in time and associated thermal stresses, Journal of Thermal Stresses, 39(11), pp. 1442-1450.
[18] Povstenko, Y., (2024), Fractional Thermoelasticity, Second edition, Springer, Cham.
[19] Povstenko, Y. and Ostoja-Starzewski, M., (2021), Doppler effect described by the solutions of the Cattaneo telegraph equation, Acta mechanica, 232, pp. 725-740.
[20] Povstenko, Y. and Ostoja-Starzewski, M., (2022), Fractional telegraph equation under moving time-harmonic impact, International journal of heat and mass transfer, 182, p. 121958.
[21] Povstenko, Y., Ostoja-Starzewski, M. and Kyrylych, T., (2023), Telegraph equation in polar coordinates: Unbounded domain with moving time-harmonic source, International Journal of Heat and Mass Transfer, 207, p. 124013.
[22] Podlubny, I., (1999), Fractional differential equations (san diego, ca: Academic).
[23] Vernotte, P., (1961), Some possible complications in the phenomena of thermal conduction, Compte Rendus, 252(1), pp. 2190-2191.
[24] Vrentas, J. S. and Vrentas, C. M., (2016), Diffusion and mass transfer, CRC Press.
[25] Zhu, Y., (2016), Heat-loss modified Angstrom method for simultaneous measurements of thermal diffusivity and conductivity of graphite sheets: The origins of heat loss in Angstrom method, International Journal of Heat and Mass Transfer, 92, pp. 784-791.

Vinayak S. Kulkarni is currently working as a Professor at the Department of Mathematics, University of Mumbai, Mumbai. His research areas are Mechanics of deformable solids, Heat and mass transfer, Partial differential equations, Boundary value problems in heat conduction, Integral transforms, Applied analysis, Applied numerical analysis, etc. https://orcid.org/0000-0002-2507-4458

Sagar Ningonda Sankeshwari is currently working as an Assistant Professor of Mathematics at School of Mathematics, Applied Statistics and Analytics, NMIMS Deemed to be University, Navi Mumbai. His research interests are Fractional thermoelasticity, Partial differential equations, etc.